

Hole formation induced by 488.0-nm light in 10- μm -thick amorphous as-evaporated As_2S_3 films

Olli Nordman* and Nina Nordman

Optical Sciences Center, University of Arizona, Tucson, Arizona 85721

(Received 30 November 1998)

When As_2S_3 films, evaporated on glass substrates, were illuminated with an intense 488-nm Ar laser beam, the two opposite beam directions (light entering the substrate first and light entering the film first) led to different hole formation characteristics. The two processes are controlled by the viscous flow of As_2S_3 with the activation energies of 0.81 and 1.10 eV. The difference in the hole formation mechanisms is based on the small penetration depth of light compared to the film thickness and on the different viscosities of exposed and unexposed As_2S_3 . Specific oscillations in the transmission curves are explained to be caused by the photoinduced anisotropic microcrystallization followed by thermal crystalline clustering. [S0163-1829(99)03428-1]

I. INTRODUCTION

Optical properties of amorphous As_2S_3 semiconductor films change when they are exposed by light with photon energy exceeding the band-gap energy E_g [$E_g = 2.39$ eV (Ref. 1)]. These so-called photostructural changes (PSC) may be reversible² or irreversible.³ For instance, light may shift the absorption edge of the films towards longer wavelengths. This phenomenon is called photodarkening. Usually photodarkening in As_2S_3 is induced by the green Ar laser line (wavelength $\lambda = 514.5$ nm, $E = 2.41$ eV) and probed by the red HeNe laser line (632.8 nm, 1.96 eV). However, even weak probing with sub-band-gap light may have an influence on As_2S_3 by generating and orientating D^- and D^+ centers.⁴ Sub-band-gap light can also change the fluidity of As_2S_3 .⁵ Intense HeNe laser light beam is found to even increase the thickness of the film.⁶ This property is used for the preparing of small lenses.⁷ Other possibilities for the optical microfabrication based on the athermal photoinduced fluidity are studied in Ref. 5. The possibility to use amorphous thin films as binary memory units has also gained interest.^{8,9} In these experiments focused laser beams are used to create holes in chalcogenide films. Hole formation is a thermal process based mainly on the change of viscosity. Surface tension gradient acts as a driving force.

In many applications mentioned above intense laser beams are used to induce PSC. The response of the film is observed in the transmission mode. Therefore, the substrate material must be transparent for the laser beams. This work verifies that if the penetration depth of the light is small compared to the film thickness, there is a difference in PSC (and hole formation) depending on the direction of the incoming beam (whether it first enters the substrate or the film). This fact is not so well recognized. In fact, we have not found any other publications for transparent substrate-chalcogenide system concerning the same subject not to speak about the similar results. Some of the earlier publications (see, e.g., Ref. 10) do show that PSC in As_2S_3 are greatly dependent on the exposing wavelength near the band gap (blue 488.0 nm and green 514.5 nm lines of Ar laser). The present paper also verifies that even unfocused laser beams with quite moderate intensities can induce As_2S_3 mass flow from the beam center towards lower exposed film areas.

This phenomenon caused by surface tension is much more prominent than the evaporation of the material. We will also give a qualitative explanation for the beam-direction-dependent behavior.

II. EXPERIMENTAL DETAILS

As evaporated amorphous As_2S_3 films with the thickness $d = 10$ μm were used for the experiments. Films were evaporated on glass substrates and stored at room temperature in the dark for more than two years. Therefore, films could be regarded as thermally relaxed.³ The history of the films is better explained in Ref. 11.

To induce PSC films were illuminated with the blue, vertically polarized 488.0 nm (2.54 eV) Ar laser line. The blue line was chosen, because its absorption coefficient (α) in As_2S_3 films is higher than that of the green line. Therefore, the penetration depth (d_p) ($\propto \alpha^{-1}$) of the blue line is shorter, which ensured the desired maximum difference between the film thickness and d_p . We used a Gaussian shape, unfocused laser beam with $1/e^2$ radius ($r_0 = 0.75$ nm). Thus, the power distribution can be expressed as

$$P_r(r) = P_0 e^{-2(r/r_0)^2}, \quad (1)$$

where r is the distance from the beam center and P_0 is the peak power on the surface of the film. We have subtracted losses caused by reflections when P_0 is given (air-glass interface 4.0%, glass-film interface 6.3%, air-film interface 18.4%).

Optical density (OD) is defined as

$$D = \log_{10} \left(\frac{P_0}{P_T} \right), \quad (2)$$

where P_T is the transmitted laser beam power. P_T was recorded using a computer. The interval between the successive measuring points was 60 ms.

The profiles of the holes were measured by Tencor Alpha-Step[®] 500 Surface Profilometer.

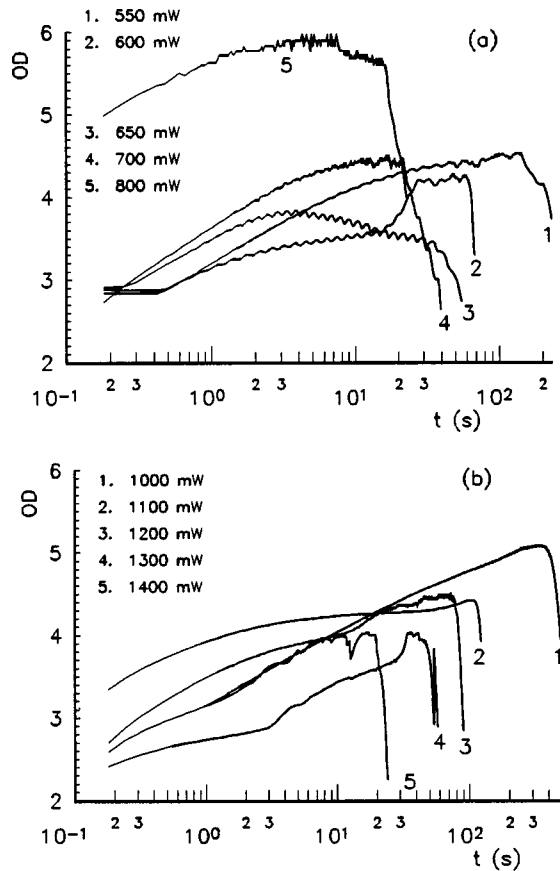


FIG. 1. Optical density as a function of the exposure time (t) with different laser beam powers (P_0) (displayed in the legend). (a) The laser beam enters the film through glass substrate. (b) The laser beam enters directly the film.

III. RESULTS

Figure 1(a) shows OD as a function of the exposure time. In this case the light entered the film through the glass substrate. Laser beam powers (P_0) are displayed in the figure. The given power range covers the whole hole opening area that was reasonable in our experiments. When laser power was 500 mW the hole did not open within 20 min. When laser power exceeded 800 mW the opening process was so fast that we could not reliably record it (compare 800 mW).

According to Fig. 1(a) in the beginning of the exposure $OD \approx 2.5$. Therefore, the initial absorption coefficient α_0 of As_2S_3 film is $5.7 \times 10^3 \text{ cm}^{-1}$. This means that the power drops to $1/e$ part from its initial value at $z = 1.7 \mu\text{m}$ (z is the position coordinate inside the film in the direction of the beam). Generally OD is increasing with the exposure time. This is due to the photodarkening effect. However, curve 3 and partially curve 2 make an exception. Curves 1–3 also have an oscillatory behavior. These facts are closer studied in Discussion. The opening of the hole is seen as a sudden drop of OD at the end of the curves.

Figure 1(b) displays the OD curves when the light enters the film first. As can be seen the powers needed for the hole opening are greater than in previous case [Fig. 1(a)]. Also the hole opening times (t_0) are longer. This is due to the fact that when the beam hits the film PSC occur. The surface of the film is photodarkened. It means that the structure of As_2S_3 is polymerized (see for example Ref. 3). The viscosity

is increased. It is later shown that the activation energy governing the viscosity also increases. When the light enters the film through the glass substrate only a small fraction of quanta can reach the film-air boundary where the hole forming process starts. Thus the hole forming process in this case in the beginning is dealing with unexposed or only slightly exposed As_2S_3 with lower viscosity (contrary to the other case where it has to deal with higher viscosity As_2S_3). However, in the end of the hole opening process the beam enters high viscosity, polymerized As_2S_3 . Therefore, this hole opening process is more nonlinear as the former one.

Why OD's in Figs. 1(a) and 1(b) do not differ so much even though PSC should be much more prominent in the latter case [Fig. 1(b)]? The dynamics of OD (without hole formation) is well described by Tomlinson in his theory concerning dynamics of photochromic conversion.¹² Accordingly, OD, when lower intensity is used, should be considerably smaller than OD induced by higher intensity. However, in the case of Fig. 1(b) hole formation starts from the highly exposed area. The mass moving away has high OD. Therefore, when the hole starts to form the OD is significantly reduced. Instead, when the beam enters the film through the glass substrate the As_2S_3 mass, which moves away has low OD. This reduces the difference in OD's.

Figure 2(a) shows the profile of the hole after the hole opening for $P_0 = 600 \text{ mW}$ and $t_0 = 65 \text{ s}$. The corresponding values for Fig. 2(b) are 1100 mW and 120 s, respectively. The profile of Fig. 2(b) (light enters the film first) is different from that of Fig. 2(a). The main reason for the difference are the different viscosities as already explained above.

The profiles in Fig. 2 are typical representatives of their cases. Asymmetry of the profiles is due to the gravity, which pulled the low viscosity As_2S_3 out of the hole. When low viscosity As_2S_3 is cooled down it forms a rim around the hole. The rims can clearly be seen in both figures. This fact suggests that the hole forming process is controlled by the viscosity⁹ not vaporization.

IV. DISCUSSION

Before we are able to analyze the processes further we have to know the increase of the temperature caused by the laser beam. In the middle of the Gaussian-shape laser beam the temperature is found to be^{9,13}

$$T_0(t) = \frac{P_a}{Kw\pi^{3/2}} \arctan\left(\frac{2\sqrt{Dt}}{w}\right). \quad (3)$$

In this formula, P_a is the beam power absorbed by the film (in our case $\approx P_0$), K is the thermal conductivity of the glass substrate [$1 \times 10^{-2} \text{ W/K cm}$], w is the beam waste (0.53 mm), t is the exposure time, and D is the thermal diffusivity of the glass ($5.3 \times 10^{-3} \text{ cm}^2/\text{s}$). There are several conditions which have to be fulfilled for Eq. (3) to be valid.^{9,13} (i) The film has to absorb the light not a glass substrate. This is clearly true for our system. (ii) It is assumed that the glass substrates are thick enough (compared to the film thickness) to conduct all the heat away. We used glass plates with the thickness of 3 mm. Clearly this condition is fulfilled. The condition is further supported by the fact that the heat conductivity of the glass is about ten times higher than that of

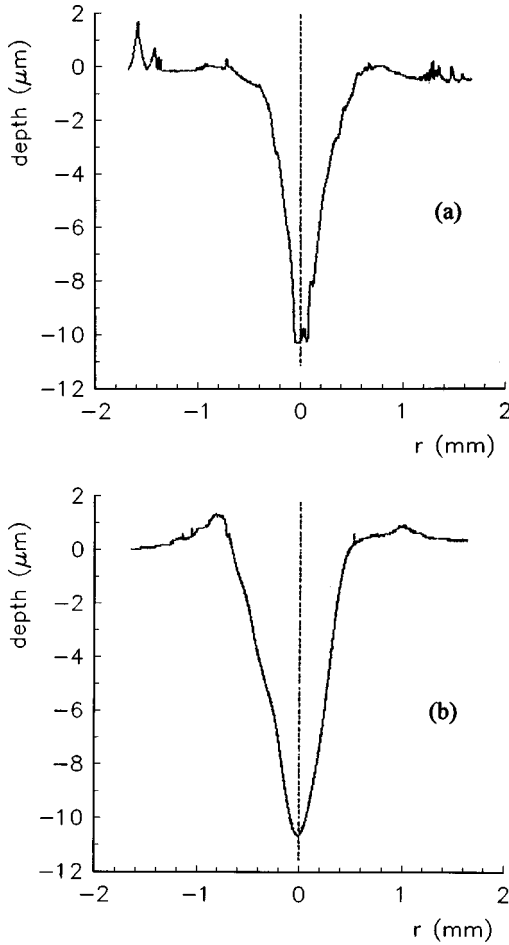


FIG. 2. Typical profiles of the holes (r is the radial distance from the laser beam center). (a) The laser beam enters the film through glass substrate ($P_0=600$ mW, $t=t_0=65$ s). (b) The laser beam enters directly the film ($P_0=1100$ mW, $t=t_0=120$ s).

As₂S₃. (iii) Radial heat diffusion effects have to vanish. This is true because the beam waist ($w=0.53$ mm) was much larger than the film thickness ($d=10$ μm). (iv) In order the temperature inside the film (in the direction of the z axis) to be constant the measurements have to be done in the time scale exceeding d^2/D_f (D_f is the thermal diffusivity of the film). In our case $d^2/D_f \approx 90$ ms [$D_f=1.1 \times 10^{-3}$ cm²/s (Refs. 13 and 14)] so also this condition is fulfilled. Accordingly, the temperature increase T_0 (t_0) ranged from 291 to 424 °C with power levels from 550 to 800 mW [Fig. 1(a)] and from 530 to 742 °C with power levels from 1000 to 1400 mW [Fig. 1(b)]. When power was higher than 1400 mW films started to boil [the boiling point of As₂S₃ natural orpiment is 707 °C (Ref. 15)]. This could be easily seen as smoke rising from the exposed area. The difference between the observed and given boiling points (762 and 707 °C) may be due to the inaccurate glass parameter (K and D) values.

For the viscosity controlled hole opening process the hole opening time can be expressed as⁹

$$t_0(T) = \frac{C}{d \nabla_r T} \exp\left(\frac{\Delta E}{kT}\right). \quad (4)$$

In this expression, C is a constant. The radial temperature gradient $\Delta_r T$ is a slowly varying function of T compared to

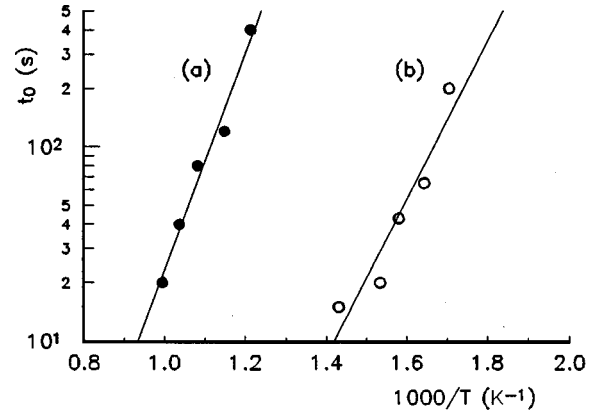


FIG. 3. Hole opening times (t_0) as a function of $1/T$ ($T=T_0+292$). (a) The laser beam enters the film through glass substrate ($\Delta E=0.81$ eV). (b) The laser beam enters directly the film ($\Delta E=1.10$ eV).

the exponential function.⁹ Therefore, it can be regarded as constant. The viscosity [$\eta(T)$], activation energy (ΔE), and absolute temperature (T) are connected together by Arrhenius-type relation

$$\eta(T) = \eta_0 \exp\left(\frac{\Delta E}{kT}\right). \quad (5)$$

By taking t_0 values from Fig. 1 and using $T=T_0+292$ we have drawn Fig. 3, where t_0 is displayed as a function of $1/T$. Using Eq. (4) we have derived ΔE values 0.81 eV [Fig. 1(a)] and 1.10 eV [Fig. 1(b)]. These two different values show that viscosities do depend on the direction of incoming laser beam. Chauemy, Fornazero, and Mackowski¹⁶ measured $\Delta E=1.11$ eV for the unexposed As₂S₃. One reason for our lower values could be that we do not investigate the photodecomposition of As₂S₃ (light-enhanced vaporization connected to the role of oxygen¹⁷⁻²¹). However, if photodecomposition would have reduced the film thickness it would have increased t_0 [$t_0 \propto 1/d$, Eq. (4)] and thus, also ΔE . We think, that the greatest inaccuracies (all together approximately $\pm 20\%$) are due to the inaccurate glass parameter values (when calculating T_0) and the definition of t_0 values [Figs. 1(a) and 1(b)].

In order to get more information about the connection between the hole shape (Fig. 2) and viscosity we have redrawn the left-hand side of Fig. 2(a) and the right-hand side of Fig. 2(b) in Fig. 4. Accordingly, the profiles have different shapes. The thickness starts to change when $r < 0.5$ mm with $T_r \approx 170$ °C [Fig. 2(a)] and 290 °C [Fig. 2(b)]. In addition to the hole profiles Fig. 4 shows the radial change of temperature (T_r). It has an expression^{9,22}

$$T_r(t) = T_0(t) \exp\left(\frac{-r^2}{2w^2}\right) I_0\left(\frac{r^2}{2w^2}\right), \quad (6)$$

where I_0 is the modified Bessel function of zero order. The curve has been drawn at the moment of the hole opening [Fig. 2(a): $t_0=65$ s, $T_0=309$ °C; Fig. 2(b): $t_0=120$ s, $T_0=571$ °C]. The profile of the laser beam power P_r/P_0 [Eq.

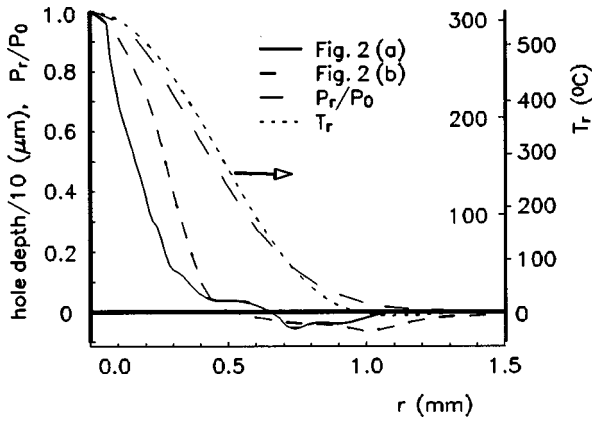


FIG. 4. Redrawn profiles from Fig. 2 [solid line, Fig. 2(a), short-dash line, Fig. 2(b)]. The power profile of the laser beam [Eq. (1)] (medium-dash line, P_r/P_0). The radial temperature distribution (tiny-dash line, T_r). T_r values should be read from the right y axis, where the lower scale is for the profile of Fig. 2(a) and the higher scale is for the profile of Fig. 2(b).

[1]) is also in the figure. We will need this curve later. Surprisingly, the last two curves have almost the similar shape as a function of r .

The viscosity ratio η/η_0 as a function of r for $\Delta E = 0.81$ and 1.10 eV is displayed in Fig. 5. The viscosities have been estimated from Eq. (5) using $T = 292^\circ\text{C} + T_r$ [T_r derived from Eq. (6)]. Accordingly, in spite of the higher temperature, the average viscosity in the second case (laser beam enters directly the film) is almost as high as in the first case (laser beam enters the film through the substrate) when $r < 0.35$ mm. This confirms our conclusion about the crosslinking of As_2S_3 , which increases the viscosity. When $r > 0.4$ mm the viscosity in the second case even exceeds the viscosity of the first case. This is due to the radial temperature difference between two cases. It becomes smaller with increasing r and the viscosity of highly exposed As_2S_3 exceeds that of slightly exposed As_2S_3 .

It is also of interest to know the connection between the viscosity [η/η_0 , Eq. (5)] and the depth of the hole (z_h) (on the surface of the hole) at the time of the hole opening (t_0). Therefore, we made use of Figs. 4 and 5 and took the η and z_h values from the figures using the same r values. Results

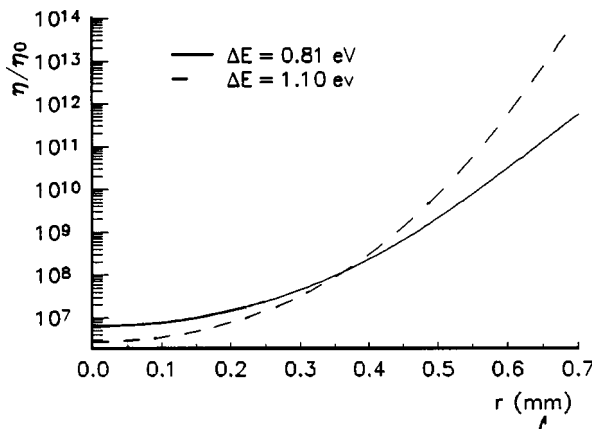


FIG. 5. The viscosity ratio η/η_0 [Eq. (5)] as a function of r (solid line, $\Delta E = 0.81$ eV, short-dash line, $\Delta E = 1.10$ eV).

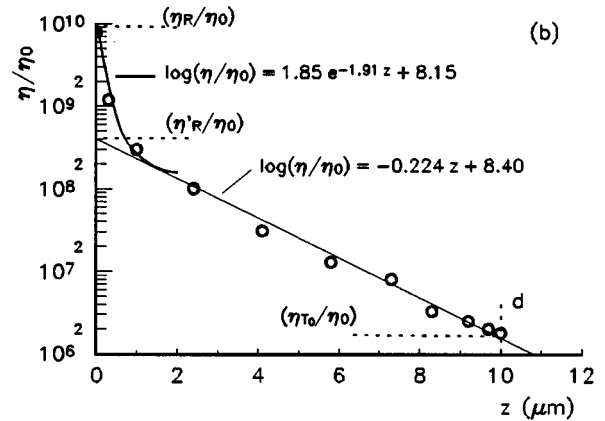
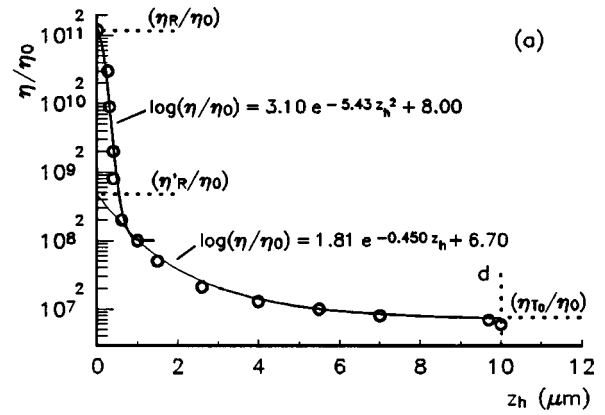


FIG. 6. The viscosity ratio η/η_0 on the surface of the hole [Eq. (5)] as a function of the hole depth (z_h). Symbols (open circles) represent sampling points (different r values). The fits to the sampling points are given in the figure. (a) The laser beam enters the film through glass substrate. (b) The laser beam enters directly the film.

are seen in in Figs. 6(a) and 6(b). Our sampling points (representing different r values) are seen as open circles. We have made two fits in both figures based on the acquired points. The fits are given in the figure. When the laser beam enters the film through the glass substrate [Fig. 6(a)] the fit deeper in the hole ($z_h > 1.0 \mu\text{m}$) is of the form $\log(\eta/\eta_0) = a \exp(-bz_h) + c$. This gives us

$$\eta = \eta_s \exp[a \exp(-bz_h)]$$

with

$$a = \ln\left(\frac{\eta'_R}{\eta_s}\right), \quad b = -\frac{1}{d} \ln\left\{\ln\left(\frac{\eta_{T_0}}{\eta_s}\right) \left[\ln\left(\frac{\eta'_R}{\eta_s}\right)\right]^{-1}\right\},$$

$$c = \ln\left(\frac{\eta_s}{\eta_0}\right). \quad (7)$$

In this expression η'_R is the viscosity where exponential function intersects the η/η_0 axis [see Fig. 6(a)], η_s is the viscosity value at $z_h = \infty$ (defined by the exponential function) and η_{T_0} is the viscosity at the beam center. When $0 < z_h < 1.0 \mu\text{m}$ (near the rim) the fit is of the form $\log(\eta/\eta_0) = a \exp(-bz_h^2) + c$. The intersection of the function and η/η_0 axis is marked as (η_R/η_0) where η_R is the viscosity at the edge of the rim.

According to Fig. 6(b) (the laser beam enters the film first) the $\log(\eta/\eta_0)-z_h$ dependence inside the hole ($z > 1.5 \mu\text{m}$) has a simple form $\log(\eta/\eta_0)=az_h+b$. Taking into account that $b=(\eta'_R/\eta_0)$ we get for the viscosity

$$\eta = \eta'_R \exp\left(\frac{a}{d}z_h\right),$$

where

$$a = \ln\left(\frac{\eta_{T_0}}{\eta'_R}\right). \quad (8)$$

The viscosity seems to be exponentially related (with $a < 0$) to the hole depth. Near the rim ($0 < z_h < 1.5 \mu\text{m}$) the $\log(\eta/\eta_0)-z_h$ dependence has the form $\log(\eta/\eta_0)=az_h+b$. This leads to the same kind of dependence as given by Eq. (7), however, with different constants.

By comparing previous results we can draw the conclusion that the hole forming process in the case where the beam hits directly the film [Fig. 6(b)] is more linear than in the case, where the beam enters the film through the substrate [Fig. 6(a)]. It is also obvious if we think the viscosities are different as already explained.

What causes the peculiar oscillations of OD in Fig. 1(a) (curves 1–3)? The mechanism that is based on hot, laser beam-induced electrons and on thermally activated atomic transitions between metastable states is known to cause oscillations.²³ However, our oscillations are far too regular to be caused by the same effect. In addition oscillations clearly are due to thermal effects, which is not the case when we are dealing with hot electrons. So we can exclude this phenomenon. It is not caused by interference either, because the oscillations amplitudes are too large. They correspond about 18% transmittance change in the nonabsorbing material. Neither they cannot be caused by spurious reflectance gratings, because the film is in continuous movement in exposed area already in the beginning of the exposure. We suggest that oscillations are due to the phase transition from the amorphous state to the crystalline state. Clusters of microcrystals are formed through the photoinduced crystallization assisted by the heat from the laser beam.²⁴ These clusters are oriented according to the incoming laser beam polarization.

To investigate the situation more closely we have redrawn the curves 1–3 from Fig. 1(a) to Fig. 7 with their corresponding temperatures at the center of the beam [Eq. (3)]. According to Ref. 24 photoinduced anisotropy is the manifestation of photoelectronic-stimulated crystalline growth. Photoinduced anisotropy in As_2S_3 has a maximum near the room temperature and it sustains at least up to 100°C .²⁴ It is quite reasonable to assume that clusters formed by the photoinduced crystalline growth remain up to the As_2S_3 melting temperature $T_m = 327^\circ\text{C}$.^{25,26} It is also assumed that optical absorption is decreased with the cluster size.

From curve 1 in Fig. 7 we see that the first oscillations appear when temperature in the middle of the beam is $\approx 280^\circ\text{C}$. As a consequence OD decreases. However, increasing temperature destroys the clusters and OD starts to rise. Meanwhile, the temperature where the first oscillation appeared has moved away from the beam center (see Fig. 4). Clusters start to form away from the beam center. This pro-

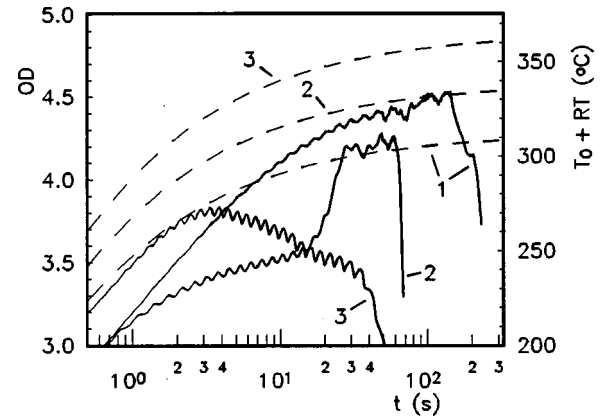


FIG. 7. Redrawn curves 1–3 (solid line) from Fig. 1(a). Laser beam-induced temperature ($T_0 + \text{RT}$, RT is room temperature) (short-dash line) as a function of the exposing time (t) (for curves 1–3) can be read from the right y axis.

cess needs certain amount of energy (laser beam exposure) before OD starts to go down again. Therefore, OD oscillations are caused by the the ring of the crystalline clusters, which moves away from the beam center with the exposure time.

Curve 2 in Fig. 7 shows a sudden overall increase in OD at temperature $T_0 \approx 320^\circ\text{C}$. The reason to this increase is hard to explain because curve 3 (with higher temperature) contains OD oscillations during the whole hole opening process. Perhaps it is because of intensity, which in the latter case is a little bit higher. Anyway, the oscillations depend on temperature that is a function of the position (r), exposure time and light intensity inside the sample. Light intensity itself is a function of the position and exposure time (see Fig. 4). Dependences are thus rather complicated and not so easy to predict.

Curves 4 and 5 in Fig. 1(a) do not show oscillations because the temperature is too high for the crystalline clusters to form.

V. CONCLUSIONS

Activation energies for the hole opening were found to be different depending on the direction of the exposing laser beam. When the light enters directly the film PSC polymerize the surface where the hole-opening process starts. Viscosity on the surface increases. The hole opening, therefore, happens in the area of high viscosity already from the beginning. When the light enters the film through the glass substrate only a small fraction of photons can reach the film-air boundary. Thus the hole forming process in this case, in the beginning, is dealing with unexposed or only slightly exposed As_2S_3 . However, in the end of the hole opening process the light has to face high viscosity, polymerized As_2S_3 . Therefore, this hole opening process is more nonlinear as the former one.

Due to the different nature of the beam-direction-dependent hole processes also the profiles of the holes were different. In the nonlinear case (beam enters the film through substrate) also the profiles were more complex than in other case. When the laser beam exposed directly the film the profile inside the hole was found to be exponential function of

hole depth. Near the edge the profile was estimated to be of the form $\exp[\exp(-bz_i)]$, where b is a constant.

The observed quite regular oscillations in some OD- t curves were explained to be caused by the photoinduced microcrystallization. These crystals are optically anisotropic. With increasing exposure (temperature) these microcrystals serve as nuclei for crystalline clusters. These clusters vanish when temperature is near the melting point. Clusters decrease OD and their destruction increase OD. The oscillations may appear when temperature (function of laser beam intensity, position, and exposure time) and light intensity inside the film (function of the position and exposure time) are in favor for cluster forming and destruction simultaneously. The appearance of the oscillation was explained as a cluster ring, which moves away from the beam center with increasing exposure.

We feel that the method and acquired results are useful also for other investigators. The method is simple and easy to use. It gives direct information about the viscous behavior of the material as a function exposing wavelength and exposure. In this paper we studied amorphous, as evaporated, aged As_2S_3 films. The method can be applied also to different kinds of As_2S_3 films and to other chalcogenides including As-Se system.¹¹ However, results may differ much because physical properties of chalcogenides may change drastically even as a function of the composition.¹¹ This paper clearly shows that beam-direction-dependent behavior exists and it has to be taken into account under conditions similar to this work. It also shows that care should be taken if even moderate power unfocused laser beams are used. They may induce film material transfer from higher exposed parts to lower exposed regions.

*FAX: (520) 621-4442. Electronic address: onordman@u.arizona.edu

¹J. B. Ramirez-Malo, E. Marquez, P. Villares, and R. Jimenez-Garay, *Phys. Status Solidi A* **133**, 499 (1992).

²G. Pfeiffer, M. A. Paesler, and S. C. Agarwal, *J. Non-Cryst. Solids* **130**, 111 (1991).

³A. Ozols, O. Salminen, and M. Reinfeld, *J. Appl. Phys.* **75**, 3326 (1994).

⁴A. Ozols, N. Nordman, O. Nordman, and P. Riihola, *Phys. Rev. B* **55**, 14 236 (1997).

⁵H. Hisakuni and K. Tanaka, *Science* **270**, 974 (1995).

⁶H. Hisakuni and K. Tanaka, *Appl. Phys. Lett.* **65**, 2925 (1994).

⁷H. Hisakuni and K. Tanaka, *Opt. Lett.* **20**, 958 (1995).

⁸Motoyasu Terao, Kazuo Shigematsu, Masahiro Ojima, Yoshio Taniguchi, Shinkichi Horigome, and Seiji Yonezawa, *J. Appl. Phys.* **50**, 6881 (1979).

⁹A. Blatter and C. Ortiz, *J. Appl. Phys.* **73**, 8552 (1993).

¹⁰O. Salminen, N. Nordman, P. Riihola, and A. Ozols, *Opt. Commun.* **116**, 310 (1995).

¹¹O. Nordman, N. Nordman, and N. Peyghambarian, *J. Appl. Phys.* **84**, 6055 (1998).

¹²W. J. Tomlinson, *Appl. Opt.* **15**, 821 (1976).

¹³H. S. Carslaw and J. C. Jaeger, *Conduction of Heat in Solids*, 2nd

ed. (Oxford University Press, Cambridge, England, 1959).

¹⁴*Handbook of Infrared Optical Materials*, edited by Paul Klocek (Dekker, New York, 1991).

¹⁵*CRC Handbook of Chemistry and Physics*, 60th ed., edited by R. C. Weast (CRC, Boca Raton, FL, 1980).

¹⁶G. Chaussemy, J. Fornazero, and J. M. Mackowski, *Phys. Chem. Liq.* **11**, 219 (1982).

¹⁷J. S. Berkes, S. W. Ing, Jr., and W. J. Hillegas, *J. Appl. Phys.* **42**, 4908 (1971).

¹⁸S. A. Keneman, *Appl. Phys. Lett.* **19**, 205 (1971).

¹⁹M. Janai and P. S. Rudman, *Photograph. Sci. Eng.* **20**, 234 (1976).

²⁰M. Janai and P. S. Rudman, *Phys. Status Solidi A* **42**, 729 (1972).

²¹L. Tichy, H. Ticha, P. Nagels, and E. Sleetx, *Opt. Mater.* **4**, 771 (1995).

²²M. Lax, *Appl. Phys. Lett.* **33**, 786 (1978).

²³I. Abdulhalim, R. Beserman, and Yu. L. Khait, *Europhys. Lett.* **4**, 1371 (1987).

²⁴K. Tanaka and K. Ishida, *J. Non-Cryst. Solids* **227-230**, 673 (1998).

²⁵R. Zallen, *The Physics of Amorphous Solids* (Wiley, New York, 1983).

²⁶P. Pohac, A. Della Casa, and A. Gauman, *Krist. Tech.* **9**, 237 (1974).